Plasma Membrane Sorting of Muscarinic Acetylcholine Receptors

Jeffrey Justin Menrije Estella

A thesis

submitted in partial fulfillment

of the requirements for the degree of

Master of Science

University of Washington

2012

Committee:

Neil Nathanson

Edith Wang

Larry Zweifel

Program Authorized to Offer Degree:

Department of Pharmacology

TABLE OF CONTENTS

LIST OF FIGURES

LIST OF ABBREVIATIONS

mAChR----------Muscarinic acetycholine receptor

GPCR----------G-protein coupled receptor

TGN----------*Trans*-Golgi Network

AIS----------Axon initial segment

DIV----------Days *in vitro*

PBS----------Phosphate buffered saline

PBST----------Phosphate buffered saline + 0.2% Triton X-100

PCR----------Polymerase chain reaction

MDCK----------Madin-Darby Canine Kidney

BSA----------Bovine serum albumin

DMEM----------Dulbecco's modified Eagle's medium

NBA----------Neurobasal A

NBA-GM----------Neurobasal A - Growth Medium

ACKNOWLEDGEMENTS

I thank all those who have supported me throughout graduate school: my family for their unyielding love and support, my Seattle and California friends for the good times and good memories, my classmates for the banter and drinks, my labmates for their company in the ivory tower, and the Department of Pharmacology for allowing me the opportunity to do some science. I especially thank Neil Nathanson for his wisdom, experience, patience, humor, and bagels.

CHAPTER 1

Introduction

Cell Polarity

Polarity can be defined as the asymmetrical structure and organization of a cell so that cellular components are distributed unequally within the cell. Ubiquitous in both single and multi-cellular organisms, polarity is responsible for defining the specialized function of an individual cell.

Defects in polarity can result in a myriad of different disease states. Bartter's Syndrome is caused by a missorting of the inwardly rectifying potassium channel ROMK to the apical membrane of epithelia in the thick ascending Loop of Henle (Naesens et al. 2004). A loss-of-function mutation in the scaffolding protein Ankyrin B causes inherited Type 4 Long-QT Syndrome, which can result in cardiac arrhythmias (Mohler et al., 2003). Missorting of the low density lipoprotein receptor to the apical membrane of hepatocytes can cause familial hypercholesterolemia Koivisto et al., 2001). The mechanisms by which cells establish and maintain polarity remain a large focus in the field of cell biology.

The task of elucidating the mechanisms responsible for the large variety of shapes and asymmetry we see in different cells may seem daunting at first glance. However, work in the field suggests that such a variety is the result of variations of mechanistic themes common to all eukaryotic cells. First, sorting signals that are intrinsically coded in proteins are recognized by cytoplasmic trafficking complexes to deliver the protein to specific plasma membrane domains. Second, scaffolding and signaling complexes associate with the cytosolic face of different membrane regions to establish the biochemical identity of that region. And third, adhesion proteins bind the extracellular matrix and other adhesion proteins on neighboring cells to correctly orient the cell in three-dimensional space (Mellman and Nelson, 2008). There has been notable progress so far in identifying and understanding the specific variations of these mechanistic themes in highly specialized cell types. Two of the most well-understood models for understanding cellular polarity are epithelial cells and neurons.

Epithelial Cell Polarity

Perhaps one of the most-studied models of eukaryotic cell polarity is the apical-basolateral polarity of epithelial cells. Epithelial cells line the surfaces of the human respiratory, urinary, and digestive tracts as well as other organ systems where they mediate the exchange of material between the external lumen and the internal extracellular matrix. Such function is possible through the polarity of epithelial cells. Epithelial tissue is comprised of a sheet of cells interconnected by impermeable tight junctions that separate the lumen-facing apical surface from both the basement membrane-facing basal surface and the intercellular-facing lateral surfaces. This results in two functionally distinct membrane domains: the apical domain and the basolateral domain. Much of the work done to study epithelial polarity utilizes the Madin-Darby Canine Kidney (MDCK) cell line as a biological model.

Establishing polarity in an epithelial cell begins with external cues involving physical contact at discrete foci with both the extracellular matrix and other epithelial cells (Datta et al., 2011). Establishment of epithelial polarity is facilitated by three complexes named Par, Crumbs, and Scribble. Scribble is known to define the basolateral domain, with Par and Crumbs defining the apical domain (St. Johnston et al., 2010). The cytoskeletal network rearranges so that in the final polarized state, most microtubules run parallel to the apico-basal polarity axis (Bacallo et al., 2009). The formation of tight junction complexes is important for both establishing and maintaining polarity. Tight junctions act as a barrier to prevent lateral diffusion of sorted proteins and lipids between membrane domains (Yamanaka et al., 2008; van Meer et al., 1986).

Exchange of material between the lumen and the extracellular matrix is dependent upon proper sorting of functional proteins to the apical and basolateral membrane domains. The general mechanisms by which proteins are sorted into their proper domains include: direct sorting to the apical or basolateral membrane domains, transcytosis, and selective retention. Direct sorting, as the name suggests, is the sorting event in which a membrane protein with a sorting signal is sent directly to its target membrane domain. Transcytosis is a mechanism whereby a sorted protein is delivered to a membrane domain that is NOT its target domain. The protein is then rapidly endocytosed and shuttled to its final membrane

destination. Finally, selective retention is a mechanism where a protein is delivered to both the basolateral and apical surfaces, but the protein remains stable in only one membrane domain, resulting in a polarized steady-state distribution.

The trafficking of surface proteins begins at the rough endoplasmic reticulum (ER), where newly synthesized membrane proteins are inserted into the rough ER membrane and subsequently packaged into vesicles destined for the Gogli apparatus. At the most distal region of the Golgi, the trans-Golgi network (TGN), membrane proteins are sorted into transport vesicles that are targeted to their specific plasma membrane domain (Griffiths and Simons, 1986). In epithelial cells, membrane proteins can traverse apical and basolateral early endosomes, as well as apical and common recycling endosomes en route to their target membrane domain (Folsch et al., 2009; Sheff D.R., et al., 2008; Brown et al., 2000). Intrinsic sorting signals determine the final destination of a sorted protein.

Apical Sorting Signals

Apical sorting signals and the mechanisms of apical sorting are diverse, where sorting signals have been known to occur on the cytoplasmic, transmembrane, or extracellular regions of a membrane protein (Weisz et al., 2009). Apical sorting of a membrane protein can be achieved by N- or O-linked gylcosylation, association with lipid rafts, gylcosylphosphotidyl-inositol (GPI) anchors, or by amino acid sequences coded in the protein itself (Cao et al., 2012).

GPI-Anchors

Glycosylphosphotidyl-inositol (GPI) anchors were among the first apical sorting signals to be identified (Lisanti et al., 1989). GPI-anchored proteins (GPI-APs) have a domain that is linked to the outer leaflet of the lipid membrane by a glycosylated phosphatidyl inositol. Experiments demonstrate that both endogenous GPI-APs and chimeric GPI-APs are sorted apically in polarized MDCK cells (Lisanti et al., 1989; Lisanti et al., 1988). However, the strength of GPI anchors as an apical sorting signal and the mechanism by which it achieves apical sorting remains unclear. Some GPI-APs are targeted basolaterally such as GPI-anchored prion protein in MDCK cells (Sarnataro et al., 1989) and many endogenous GPI-

APs in Fischer rat thryroid epithelial cells (Zurzolo et al., 1993). It has been shown that clustering of GPI-APs is also necessary for efficient sorting to the apical surface (Hannan et al., 1993). More recent work demonstrates the importance of different GPI-attachment sequences and fatty acid remodeling in apical sorting (Paladino et al., 2008; Kinoshita et al., 2008).

N- and O-linked Glycosylation

N- and O-linked oligosaccharides have been identified as apical targeting signals. Addition of N-glycans to the basolaterally sorted Na^+/K^+-ATPase β1 subunit can redirect the protein to the apical domain in HGT-1 cells (Vagin et al., 2005). Deletion of an O-glycosylated domain of the p75 neurotrophin receptor causes this protein to switch from basolateral to apical sorting (Yeaman et al., 1997). Removing N- or O-glycans can cause an apically sorted protein to be sorted non-preferentially. While N- and O-glycans can act as an apical sorting signal, it is often recessive in the co-presence of a dominant basolateral sorting signal (Fiedler and Simons, 1995).

Amino Acid Signals

A variety of endogenous apical sorting signals have been identified in the transmembrane and cytosolic regions of apical proteins ranging from a few amino acids to up to 30 amino acid long sequences (Cao et al., 2012). The influenza virus protein hemagglutinin (HA) contains an apical sorting signal in its transmembrane domain (Scheiffele et al., 1997). Rhodopsin and the NKCC2 co-transporter both contain apical sorting signals in their C-terminal cytosolic regions (Chuang et al., 1998; Carmosino et al., 2010). Some apical sorting signals are able to confer apical sorting to otherwise basolaterally sorted proteins (Chicka and Strehler, 2003; Chmelar and Nathanson, 2006).

Lipid Rafts

The early concepts of the lipid raft idea postulated that apically targeted proteins, such as GPI-APs, are sorted by their affinity for microdomains of glycosphingolipids and cholesterol in the Golgi that act as apical transport carriers (Simons and van Meer, 1988). The concept has evolved as more recent work has broadened our understanding of the topic. Lipid rafts can now be defined as dynamic, nanometer-sized, sterol-sphingolipid-enriched, tightly packed lipid-protein assemblies that fluctuate on a

sub-second time scale (Cao et al., 2012). Much of the work done to study lipid rafts involve the apically sorted influenza virus HA protein. Various studies demonstrate that the HA protein is present in dynamic cholesterol-dependent microdomains (Cao et al., 2012). Recent work in yeast used yeast plasma membrane proteins as bait to isolate secretory vesicles and analyze their lipid composition. These studies show that secretory vesicles with GPI-anchored and membrane protein cargo are enriched with sphingolipids and ergosterol (the cholesterol equivalent in yeast) (Klemm et al., 2009; Surma et al., 2011).

Basolateral Sorting Signals

Basolateral sorting signals are not as diverse as their apical counterparts. So far, all known basolateral sorting signals are amino acid sequences coded in their respective protein in cytoplasmic regions of the protein, usually at the C-terminal tail. The first basolateral sorting signal was identified in the polymeric immunoglobulin-A receptor (pIgR) and was later shown to confer basolateral sorting to other proteins (Mostov et al., 1986; Casanova et al., 1991) .

Since then, a myriad of different basolateral signals have been identified, with a few classical sorting sequence motifs being recognized: tyrosine motifs, single- and di-leucine motifs, and di-hydrophobic motifs surrounded by acidic amino acids (Rodriguez-Boulan et al., 2005). The classical tyrosine motifs include the YXXØ motif and the NPXY motif - where X can be any amino acid and Ø is a bulky hydrophobic amino acid (Bonifacino and Traub, 2003). A single leucine basolateral sorting signal was identified in stem cell factor that required a cluster of upstream acidic residues (Wehrle-Haller and Imhof, 2001). A dileucine basolateral sorting signal was first identified in the IgG Fc receptor (Humziker and Fumey, 1994). Many di-hydrophic motifs have been identified as well (Bonifacino and Traub, 2003).

Since many basolateral sorting signals are di-hydrophobic or resemble clathrin-dependent endocytosis motifs, it has been hypothesized that adaptor protein (AP)-clathrin complexes were important for basolateral sorting. Knockdown experiments of the clathrin heavy chain in MDCK cells disrupt sorting of most basolateral proteins but do not affect sorting of apical proteins. Also, knockdown of the

mu1B subunit of the adaptor protein AP-1B in the epithial cell line LLC-PK1 causes apical sorting of many basolaterally sorted proteins (Cao et al., 2012).

Neuronal Polarity

Neurons are among the most highly polarized mammalian cells, with two functionally and molecularly distinct domains: the axonal and somatodendritic domains. Neurons begin their life as spherical cells, gradually sprouting processes called "neurites" as they mature. These neurites typically mature into one long axon and several smaller dendrites.

The asymmetrical morphology and organization of neurons allow them to propagate information in a unidirectional manner. Chemical signals are received postsynaptically at the dendritic arbor where they elicit electric potentials that converge and traverse through the cell soma to trigger an action potential at the axon hillock. This electrical signal is propagated down the axon to the axon terminal where it is converted back into a chemical signal in the form of biochemical neurotransmitters that are released to the dendritic arbor of neighboring neurons. One aim in the field of cellular biology is to understand the molecular mechanisms that orchestrate the establishment and maintenance of neuronal polarity.

Cytoskeleton and Axonal Growth

The cellular cytoskeleton, as the name suggests, acts as the "skeleton" of a cell, conferring specific morphologies to different cell types and functioning as scaffolding for localized cellular components. Additionally, the cytoskeleton provides a physical route for trafficking of sorted proteins. The cytoskeleton is comprised of three types of polymeric structures: microfilaments, intermediate filaments, and microtubules.

The smallest of the three, microfilaments are comprised of two strands of actin filaments, known as F-actin, that together form a double helix. Strands of F-actin are comprised of individual actin subunits called G-actin. Polymerization of monomeric G-actin into F-actin strands requires nucleating factors to promote the addition of ATP-bound G-actin monomers to the leading "barbed" end of F-actin strands. Upon hydrolysis of ATP to ADP, ADP-bound G-actin causes destabilization of F-actin, promoting the

removal of individual G-actin subunits from the trailing "pointed" end of F-actin strands (Schoenenberger et al., 2011).

Microtubules are hollow tubular structures comprised of α and β tubulin heterodimers. Nucleation of a microtubule requires a ring complex at the centrosome comprised of γ tubulin. Elongation occurs as GTP-bound α and β tubulin heterodimers are added onto the γ tubulin ring complex. Shortly after polymerization, a newly-added tubulin will hydrolyze GTP into GDP. Thus, microtubules are polarized with a capped minus end and a leading plus end where elongation occurs. Microtubules undergo dynamic instability - oscillating phases of growth and shrinkage separated by phase-switching events called "catastrophe" and "rescue" (de Forges et al., 2012).

In neurons, the cytoskeleton plays an important role in extending neurites from the soma. Highly motile compartments at the tips of neurites called "growth cones" respond to extracellular cues to guide neurites – particularly the nascent axon – to their final destination within an organism (Vitriol and Zheng, 2012). A neuron's morphological transition from an immature non-polarized cell with many identical neurites into a mature polarized neuron with several dendrites and a single axon involves the dynamic turnover of growth cone actin filaments and stabilization of microtubules in the nascent axon (Witte and Bradke, 2008).

An immature spherical neuron will sprout several neurite processes that are thought to be identical. Following an initiating signal thought to originate from the centrosome, accelerated outgrowth occurs in a single neurite destined to become the axon. The growth cone of the future axon becomes more dynamic, with its actin filaments showing increased turnover while the microtubules of the future axon become more stabilized (Bradke and Dotti, 1999). In contrast, future dendrites show more stable growth cones (Witte and Bradke, 2008). Pharmacological depolymerization of actin filaments as well as pharmacological stabilization of microtubules can cause non-growing dendrites to grow into axons (Bradke and Dotti, 1999; Witte et al., 2008).

Several actin and microtubule regulating proteins have been implicated in neuronal polarity. The WAVE complex of proteins regulates actin polymerization in growth cones, promoting axon growth

(Kawano et al., 2005). Ena/VASP proteins accelerate actin polymerization in growth cones, and neurons lacking these proteins do not form neurites (Krause et al., 2003; Krause et al., 2004). Knocking down cofilin, an actin severing protein, disrupts axon formation; but expression of a constitutively active mutant of cofilin can enhance growth (Garvalov et al., 2007; Jacobs et al., 2007). MAP2 and Tau act as microtubule stabilizing proteins. Down-regulation of MAP2 inhibits neurite formation, and down-regulation of Tau inhibits axon formation (Caceres and Kosik, 1990; Caceres et al., 1992). CRMP-2 binds free tubulin subunits to promote their binding to microtubules (Fukata et al., 2002). During neuronal polarization, CRMP-2 accumulates in the future axon, and overexpression of CRMP-2 results in formation of multiple axons (Inagaki et al., 2001). These studies illustrate the importance of cytoskeletal remodeling in establishing neuronal structure and polarity.

Signaling Pathways

A number of signaling pathways have been implicated in neuronal polarity. Unsurprisingly, many of these signaling pathways involve cytoskeletal-regulating Rho GTPases such as Rac and Cdc42 (Tahirobic and Bradke, 2009). Regulation by Rho GTPases is modulated by the cycling between an inactive GDP-bound state and an active GTP-bound state where it can act upon downstream effector proteins (Jaffe and Hall, 2005). Cdc42 regulates actin dynamics in growth cones through its effectors p21-activated kinase (PAK) and WASP. PAK signaling acts on the actin cytoskeleton via cofilin (Ng and Luo, 2004). Rac1 modulates neuronal polarity by regulating formation of lamellipodia in growth cones (Ridley 2001). Rac1 acts via its two main effectors WAVE and PAK (Burridge and Wennerberg, 2004; Heasman and Ridley, 2008). Rac1 also promotes the stabilization of microtubules by inhibition of Op18, a microtubule destabilizing protein (Wittmann et al., 2004). RhoA and its downstream effector Rho-kinase (ROCK) regulate actin stability in cultured hippocampal neurons via profilin II (Da Silva et al., 2003). Furthermore, overexpression of mutant RhoA interferes with neurite outgrowth (Koh 2006).

Localization of phosphotidylinositol-3-kinase (PI3K) has been implicated in neuronal polarity and polarity of many other cell types (Arimura and Kaibuchi, 2005). PI3K has been shown to localize to the tips of stage 3 axons. Inhibition of these localized enzymes inhibits axon formation in cultural

hippocampal neurons (Shi et al., 2003). Since PI3K synthesizes phosphotidylinositol (3,4,5)-triphosphate (PIP_3), it is thought that lipid signaling is also involved as a polarization mechanism downstream of PI3K activity. One model postulates that axon-localized PI3K creates a concentrated pool of PIP_3 in axons, subsequently recruiting protein kinase B (PKB) to the cytosolic face of the axon plasma membrane. PKB inactivates glycogen synthase kinase (GSK)-3β by phosphorylation. In dendrites, GSK-3β normally inhibits the axon-forming activity of CRMP-2. So the formation of an axon by inhibition of GSK-3β is thought to occur in part by allowing CRMP-2 activity to continue locally in the nascent axon (Tahirovic and Bradke, 2009).

The Axon Initial Segment

As the name suggests, the Axon Initial Segment (AIS) is located at the most proximal area of the axon where it is thought to function as a physiological and physical barrier between the somatodendritic and axon domains (Rasband 2010). The two most identifiable features of the AIS are its fasciculated microtubule network (Palay et al., 1968) and its enrichment in voltage-gated Na^+ channels that are required to generate an action potential down the axon (Kole et al., 2008). Other proteins that are clustered to the AIS include K+ channels KCNQ2/3 and neuronal cell adhesion molecule (NrCAM) (Ogawa and Rasband, 2008). Furthermore, the AIS itself is divided into proximal and distal subdomains, with certain isoforms of ion channels expressed more proximally or distally depending on the neuron type (Grubb and Barrone, 2010).

Ankryin G (AnkG) is the main scaffold protein upon which all other AIS proteins are anchored either directly or indirectly (Grubb and Burrone, 2010). Transgenic mice that do not express AnkG do not form the AIS (Barnes and Polleux, 2009). Additionally, loss of AnkG expression abolishes the subcellular localization of its associated proteins (Rasband 2010). Little is known, however, about the mechanisms by which AnkG itself is sorted to the AIS. Although sorting of AnkG to the Nodes of Ranvier depends upon glial influence, experiments show that AIS targeting of AnkG occurs autonomously (Dzhashiashvili et al., 2007). More recent work suggests that the phosphorylated form of the inhibitor of κBα (pIκBα) plays an

upstream role in AnkG AIS sorting. Inhibition of IκB kinase (IKK) prevents phosphorylation of IκBα and causes AnkG to be retained in the soma (Sanchez-Ponce et al., 2008).

Another scaffold protein, βIV-spectrin, seems to be important for the maintenance of AIS integrity (Ogawa and Rasband, 2008). Like other members of the spectrin family of proteins, βIV-spectrin interacts with the actin cytoskeleton and also directly binds to AnkG (Yang et al., 2007). Knockout mice lacking βIV-spectrin show less stable AISs (Lacas-Gervais et al., 2004), and mutant forms of βIV-spectrin interferes with AIS targeting of voltage gated Na^+ and K^+ channels (Parkinson et al., 2001). However, it is important to note that AnkG-based AIS formation can occur in the absence of βIV-spectrin (Hedstrom et al., 2007).

The Barrier Hypothesis

The barrier hypothesis arose from the question of how neurons maintained their polarity for long periods of time - up to decades in humans - without overburdening the cell with the metabolic requirements required to constitutively sort cellular components. It was postulated that a simple barrier dividing the axonal and somatodendritic domains would be a simpler way of maintaining neuronal polarity (Rasband, 2010). Earlier experiments to test this hypothesis involved tracking fluorescently labeled membrane phospholipids. Such phospholipids that were inserted into the axonal plasma membrane would diffuse throughout the axon but would not enter the somatodendritic plasma membrane (Kobayashi et al., 1992). Later experiments would demonstrate that lateral diffusion of phospholipids was blocked at the AIS (Nakada et al., 2003). The same holds true for axonal membrane proteins such as NCAM-L1(Winckler et al., 1999). Furthermore, cytoplasmic proteins such the somatodendritic MAP2 protein are barred from crossing into the axoplasm at the AIS. Recent studies by Song and colleagues demonstrate the existence of a cytoplasmic barrier. Fluorescently labeled dextrans were loaded into the soma of cultured hippocampal neurons. Dextrans of low molecular weight (10kD) diffused evenly throughout the entire neuron while dextrans of high molecular weight (70kD) were excluded from the

axon. Additionally, they showed that transport vesicles carrying dendritic proteins were also excluded from the axon (Song et al., 2009).

A few studies have given us insight into the molecular components of the barrier. Disruption of the actin cytoskeleton allows high molecular weight dextrans to pass through the AIS (Song et al., 2009) and abolishes the polarity of some polarized membrane proteins (Winckler et al., 1999). Knockout mice lacking βIV-spectrin show impaired axonal polarization (Nishimura et al., 2007). In mature hippocampal neurons where AnkG expression is silenced, somatodendritic proteins MAP2 and the KCC2 transporter had begun to leak into the former axon, and the former axon began developing dendritic spines that were enriched in the postsynaptic marker PSD95 (Hedstrom et al., 2008). These studies suggest that the AIS and its components are important for maintenance of the barrier.

Sorting of Muscarinic Acetylcholine Receptors

Muscarinic acetylcholine receptors (mAChRs) are part of the large superfamily of seven transmembrane G-protein coupled receptors. There are five distinct muscarinic receptor subtypes: M_1-M_5 (Caulfield and Birdsall, 1998). mAChRs are expressed in the central and peripheral nervous systems, cardiac and smooth muscles, and many other cells types. Activation of mAChRs mediates a variety of cellular and physiological responses by coupling with heterotrimeric guanine nucleotide regulatory proteins (G-proteins). The M_1, M_3, and M_5 receptor subtypes generally couple to the pertussis toxin-insensitive $G\alpha_{q/11}$/ $G\alpha_{13}$ G-protein subtypes to activate phospholipase C (PLC). The M_2 and M_4 receptor subtypes generally couple to the pertussis toxin-sensitive G_i /G_o G-protein subtypes to inhibit adenylyl cyclase (AC) (van Koppen, 2003). Additionally, M_2/M_4 can regulate the activation of inwardly rectifying potassium channels through second messenger -dependent and -independent mechanisms (Pfaffinger et al., 1985) (Wickman and Clapham, 1995).

Trafficking of mAChRs to the Plasma Membrane

The general pathways for synthesis and trafficking of membrane proteins have been studied extensively. Membrane proteins are first sythesized by ribosomes on the surface of the rough endoplasmic reticulum (ER) and inserted into the ER membrane by the Sec61 complex (Rapoport, 2007). The protein

is then packaged into coatomer protein complex II (COPII)-containing vesicles and transported to the Golgi. Transport through the Golgi relies on COPI-containing vesicles that shuttle the protein through the Golgi to the trans-Golgi network (TGN) where the protein is then sent to the plasma membrane surface (Mellman and Nelson, 2008).

Transport to and retention of mAChRs at the plasma membrane surface depends highly on receptor subtype and the cell type expressing the receptor. Epitope-tagged M2 receptors expressed in CHO cells are found almost exclusively at the cell surface (Tsuga et al., 1998). Cloned M1 and M2 receptors expressed in Y1 adrenal cells were all essentially located on the cell surface (Scherer and Nathanson, 1989). The M1 receptor is expressed mostly at the surface of HEK293 cells, with some receptors retained intracellularly (Tolbert and Lameh, 1996). The M4 receptor is found primarily on the cell membrane of medium spiny neurons but is localized primarily in the cytoplasm of cholinergic interneurons (Bernard et al., 1999). Furthermore, like other GPCRs, agonist stimulation of surface mAChRs causes receptor internalization via clathrin-coated vesicles and degradation (Klein et al., 1979; Tolbert and Lameh, 1996).

Not many proteins that regulate the trafficking of mAChRs have been identified. ARF6, a small G-protein, has been implicated in the biosynthesis of mAChR internalization and the biosynthesis of M_2 and other GPCRs. Transient overexpression of a constitutively active ARF6 in HEK293 cells impairs M_2 trafficking from the ER to the Golgi (Madziva and Birnbaumer, 2006). The ER membrane protein DriP78 regulates the export of GPCRs by binding to hydrophobic motif FxxxFxxxF (where x is any amino acid) on the C-terminal of GPCRs. Overexpression of DriP78 regulates the surface expression of the M_2 receptor (Bermak et al., 2001).

Dimerization of GPCRs have implications on receptor-ligand binding, activation, and signaling (Breitwieser, 2004). The $GABA_{B1}$ and $GABA_{B2}$ receptors must dimerize in order to be targeted to the cell surface (Kaupmann et al., 1998). Homodimerization of the β2 adrenergic receptor is important for its export from the ER (Salahpour et al., 2004). Different subtypes of mAChRs have been shown to both

homodimerize and heterodimerize (Goin and Nathanson, 2006), but the role of dimerization in cell surface trafficking for mAChRs has yet to be characterized.

Subcellular Localization and Sorting of mAChRs

Muscarinic receptors have been shown to show differential targeting in many different types of polarized cells. In pancreatic acinar cells, immunofluorescence shows localization of M_3 to the lateral edge of the apical domain (Shin et al., 2001**;** Li et al., 2004). In *Xenopus* oocytes, response to muscarinic agonists was more sensitive to stimulation at the animal pole compared to the vegetal pole due to polarization of mAChRs (Matus-Leibovitch, 1990). In MDCK cells, the M_1, M_3, and M_4 receptors show basolateral sorting, while the M_2 receptor shows apical sorting, and the M_5 receptor showing non-preferential sorting to either the apical or basolateral domains (Nadler and Nathanson, 2001; Chmelar and Nathanson, 2006; Shmuel et al., 2007) . In hippocampal pyramidal cells, the M_1 and M_3 receptors are localized to cell soma and dendrites (Levey et al., 1995). In the cortex and striatum, the M_1 receptor is localized to the cell body and neurites (Levey et al., 1991).

Previous work in the Nathanson Lab has identified two sorting sequences for mAChRs. By expressing M_2/M_3 chimeric receptor constructs in MDCK cells, Iverson et al. (2005) identified a seven-amino acid sequence in the third intracellular loop (i3) of the M_3 receptor from A^{275}-V^{281} that confers basolateral sorting to the M_3 receptor. Furthermore, this amino acid sequence can also redirect the apically sorted M_2 receptor and IL-2Rα to the basolateral surface when appended to their C-terminal tails. Similarly, an apical sorting signal from the i3 of M_2 was identified by Chmelar and Nathanson (2006). Expression of a series of M_2/M_4 chimeric constructs in MDCK cells identified an eleven-amino acid sequence between I^{260}-V^{270} and a large region between Lys^{280}-Ser^{350} that are responsible for M_2 apical sorting. Deletion of both of these regions are required to abolish M_4 apical sorting, while appending the small eleven-amino acid sequence to the C-terminal of the basolaterally sorted M_4 receptor is sufficient to redirect M_4 sorting to the apical membrane.

The experiments in this thesis seek to further understand a few different aspects of plasma membrane sorting of muscarinic acetylcholine receptors. First, preliminary data from Reneé Chmelar suggests an axonal exclusion of an epitope-tagged M_1 receptor in cultured cortical neurons (Chmelar, unpublished). Confirmation of this data using axonal and somatodendritic markers was attempted. Second, the effects of mAChR dimerization on receptor surface trafficking are explored in MDCK II cells.

CHAPTER 2

Sorting of the M_1 and M_2 Muscarinic Acetylcholine Receptors in Cortical Neurons

Introduction

Cellular polarity allows neurons to propagate information in a unidirectional matter. Chemical signals in the form of various biochemical neurotransmitters are received by the dendritic arbor. Binding of neurotransmitters to membrane receptors generate either inhibitory postysynaptic potentials (IPSPs) that reinforce the hyperpolarized state of the resting membrane potential or excitatory postsynaptic potentials (EPSPs) that can collectively raise the membrane potential to threshold and subsequently generate an electrical signal in the form of an action potential. An action potential begins at the axon hillock and traverses to the distal end of the axon. At the axon terminal, an action potential is converted back into a chemical signal by causing fusion of vesicles to the presynaptic membrane, releasing neurotransmitter into the synapse. This unidirectional propagation of information relies on an asymmetrical cellular structure and a strategic distribution of cellular components such as ion channels and neurotransmitter receptors. Neuronal polarity is characterized by two functionally distinct cellular domains: the somatodendritic domain and the axonal domain.

Muscarinic acetylcholine receptors (mAChRs) have been shown to be differentially distributed depending on receptor subtype and cell type. *Xenopus* oocytes are divided into animal and vegetal hemispheres, with mAChRs located primarily on the animal hemisphere (Matus-Leibovitch, 1990). Application of acetylcholine to the serosal membrane of canine lingual epithelia elicits and electrophysiological response, but this response was not seen when acetylcholine was applied to the mucosal membrane (Simon and Baggett, 1992). In Madin-Darby canine kidney (MDCK) cells, epitope-tagged M_1, M_3, and M_4 receptors show localization to the basolateral surface while the M_2 receptor shows localization to the apical surface (Nadler and Nathanson, 2001; Chmelar and Nathanson 2006). In hippocampal neurons, the M_1 and M_3 receptors are found in the soma and dendrites (Levey et al., 1995).

The M_2 receptor can be located either presynaptically as autoinhibitory receptors in motor neurons and myenteric neurons of the ileum (Parnas et al., 2005; Takeuchi et al., 2005) or postsynaptically in GABAergic neurons of the cat visual cortex (Erisir et al., 2001).

Preliminary immunofluorescence data suggests that in cortical neurons from neonatal mice, the M_1 receptor seems to be localized somatodendritically while being excluded from the axon. In contrast the M_2 receptor seems to not be preferentially sorted to either the somatodendritic of axonal domains (Reneé Chmelar, unpublished). However, these fluorescent images are not stained for any somatodendritic or axonal markers for comparison. In this study, we attempt to repeat these experiments using immunofluorescence to visualize the somatodendritic marker MAP2 and axonal marker Tau1 in spatial relation to exogenously expressed FLAG-tagged M_1 and M_2 receptors.

Experimental Procedures

Primary Cortical Neuron Culture – Procedures for primary cortical neuron culture were based on a method from Guy Chan, Department of Pharmacology, University of Washington. Time pregnant C57B6 female mice were obtained from Charles River Laboratories International, Inc. 2-well glass chamber slides (Thermo Scientific) were coated with 100ug/mL Poly-D-Lysine overnight at 37°C in 5% CO_2. One litter of P0 neonatal pups (about 6-12 pups) were used for each set of cultures. The cortex was removed and immediately placed in dissociation media (82mM Na_2SO_4, 30mM K_2SO_4, 5.8mM $MgCl_2$, 0.25mM $CaCl_2$, 1.5mM HEPES, 20mM Dextrose, 0.001% Phenol Red, 9.5mM kynurenic acid) in aseptic conditions in a laminar flow tissue culture hood. All cortex tissues were pooled and incubated in a 10 units/mL papain solution diluted in dissociation media for 15 minutes in a 37°C water bath. During the incubation, the Poly-D-Lysine was aspirated off the chamber slides and washed once with sterile water. Following incubation, the papain solution was aspirated, and the cortex tissues were washed three times with fresh dissociation media. The tissues were then washed twice in Neurobasal A medium (Gibco-BRL). Next, the tissues were triturated twice with 5mL Neurobasal A medium to dissociate neurons from tissues. The 10mL of suspended neurons were distributed onto the chamber slides at a density of $1.5x10^6$

cells per chamber. The cells were allowed to settle for 1.5 hours before replacing the media in each chamber with 1mL of Neurobasal A Growth Medium (NBA-GM) (Neurobasal A with B27 supplement, 100 units/mL penicillin G, 0.1mg/mL streptomycin sulfate, and 0.5mM L-Glutamine). Neurons were kept in a 5% CO_2 incubator at 37°C overnight. The next day, arabinofuranosyl C was added to each chamber to a final concentration of 5mM. 50% of Neurobasal A Growth Medium was replaced for each chamber every 3 days.

Immunocytochemistry Analysis of MAP2 and Tau1- Cell culture media was aspirated from each chamber and washed twice with phosphate buffered saline (PBS) (0.8% NaCl, 0.02% KCl, 0.12% Na_2HPO_4, 0.02% KH_2O_4, 0.01% $MgCl_2$, 0.01% $CaCl_2$, pH 7.4). Cells were then fixed with 4% PFA in PBS at room temperature for 20-30 min. Cells were washed once with PBS and then permeabilized by washing twice for 5 mins with PBST (PBS with 0.2% Triton X-100). Cells were blocked for one hour at room temperature in blocking buffer (10% goat serum, 0.1M glycine, 0.05% sodium azide, 2% BSA). Blocking buffer was aspirated, and cells were incubated overnight at 4°C, shaking gently in rabbit anti-MAP2 (Sigma-Aldrich) and mouse anti-Tau1(Millipore) diluted in blocking buffer. The next day, the primary antibody solution was removed, and each chamber was washed 3-4 times with PBST. Cells were incubated at room temperature for 3hrs with fluorescent secondary antibodies - goat anti-rabbit IgG conjugated to Alexa488 fluorophores and goat anti-mouse IgG conjugated to Alexa568 fluorophores. Cells were washed twice with PBST. Chambers were removed, and slides were mounted using one drop of Vectashield mounting media (Vector Labs) per chamber surface, a coverslip placed on top of each chamber surface, and sealed with nail polish.

Confocal Microscopy - Fluorescent images were collected using a Leica SL confocal microscope (Leica Microsystems, Inc.) using 60X oil immersion lens at the Keck Microscopy Facility at the University of Washington. Images were processed using Image J.

Cell Culture – HEK293 and HT1080 cell lines were obtained from ATCC. Cell lines were maintained in Dulbecco's modified Eagle's medium (DMEM) supplemented with 10% fetal bovine serum, 100 units/mL penicillin G and 0.1mg/mL streptomycin sulfate. Cells were incubated in a humidified 10% CO_2 environment at 37°C.

Adeno Associated Virus DNA Plasmid Constructs - The Stratagene AAV Helper-Free System was utilized for AAV production. This system consists of three plasmids: pAAV-RC, pHelper, and pAAV-IRES-hrGFP. pAAV-RC contains the AAV-2 *rep* and *cap* genes encoding for replication and capsid proteins. pHelper contains the adenovirus genes VA, E2A, and E4 for high titer AAV production in HEK293 cells. pAAV-IRES-hrGFP contains a bicistronic expression cassette where a humanized recombinant green fluorescent protein is expressed from its own reading frame beginning with an internal ribosome entry site. FLAG-tagged M_1 and M_2 were constructed as described previously by Nadler et al. (2001). Briefly, mouse M_1 and porcine M_2 were cloned into the mammalian expression vector using PCR with primers coding for select restriction sites to flank the receptor coding sequences. A modified FLAG epitope was added to the extracellular N-terminal immediately following the initiator methionine. FLAG- M_1 and FLAG-M_2 were cloned into the pAAV-IRES-hrGFP plasmid previously by Reneé Chmelar using the EcoRI/XhoI restriction sites.

Adeno-Associated Virus Production – AAV production relied on cotransfection of three plasmids from the Stratagene AAV Helper-Free System. Several calcium phosphate transfection protocols were attempted, each described below.

i) The three Stratagene plasmids - pAAV-RC, pHelper, and pAAV-IRES-hrGFP containing either the FLAG-M1 or FLAG-M2 insert were co-transfected as suggested by the manufacturer (Stratagene AAV Helper-Free System). HEK293 cells were seeded into thirty 10cm tissue culture dishes at a density of $5x10^6$ cells/dish and incubated overnight in medium conditions described above. For each dish, 20 μg each of the three plasmids described above

were mixed into 1 mL of 0.3M $CaCl_2$. This solution of DNA was then mixed with 1mL of 2X HBS (pH7.1) dropwise while slowly vortexing. The mixture was then immediately added dropwise into the culture medium of each dish and incubated for 6 hours or overnight. The culture medium was then replaced with fresh DMEM and then incubated for another 72 hours.

ii) The three Stratagene plasmids - pAAV-RC, pHelper, and pAAV-IRES-hrGFP containing either the FLAG-M1 or FLAG-M2 insert were co-transfected into HEK293 cells. HEK293 cells were seeded into thirty 10cm tissue culture dishes at a density of $5x10^6$ cells/dish and incubated overnight in medium conditions described above. For each dish, 7 μg or 10 μg each of the three plasmids described above were mixed into 400 μL of a 0.25M solution of $CaCl_2$. This DNA solution was then mixed with 400 uL of a 2X HEPES solution (280mM NaCl, 50mM HEPES, 5 μM NaH_2PO_4, 10 μM Na_2HPO_4, pH 7.05) dropwise, vortexing between adding every few drops. The 800 μL mixture was then incubated at room temperature for 20 min and then added dropwise into the cell culture medium and incubated overnight. The following morning, the culture medium was replaced with fresh DMEM containing no supplements. The cultures were then incubated for another 48 hours.

Virus particles were harvested as suggested by the manufacturer (Stratagene).

AAV Titer - To determine the titer of infection, highly permissive HT1080 cells were infected as suggested by the manufacturer (Stratagene AAV Helper Free System). Briefly, $5x10^5$ HT1080 cells were plated onto 2-well glass chamber slides ($4.2cm^2$/well, Thermo Fischer Scientific) and incubated overnight. Cells were then incubated for 6 hours in AAV permissive media (DMEM supplemented with final concentrations of 40mM hydroxyurea and 1mM sodium butyrate). After incubation in permissive media, the cells were washed in L-DMEM (DMEM supplemented with 2% fetal bovine serum,100 units/mL penicillin G and 0.1mg/mL streptomycin sulfate) and incubated for 1-2 hours in 200 μL of serial dilutions of AAV stocks: 1/100, 1/1000, and 1/10000. Serial dilutions were made in L-DMEM.

After incubation, 0.5mL of H-DMEM (DMEM supplemented with 18% fetal bovine serum,100 units/mL penicillin G and 0.1mg/mL streptomycin sulfate) was added to each chamber and incubated for 40-48 hours. Following incubation, the cells were washed twice with 1X PBS and then fixed with a paraformaldehyde solution (4% w/v paraformaldehyde, 4% w/v sucrose in 1X PBS) for 20-30 min at room temperature. After fixing, cells were washed twice with 1X PBS. Chambers were removed from the slides, and slides were mounted using one drop of Vectashield mounting media (Vector Labs) per chamber surface, a coverslip placed on top of each chamber surface, and sealed with nail polish.

Calcium Phosphate Transfection of Primary Cortical Neurons - Transfection was performed on cultured cortical neurons using the primary culture technique described above. This protocol was a scaled down version of the calcium phosphate (ii) protocol described above, with a few conditions taken from a calcium phosphate transfection protocol described previously by Dudek and colleagues (2001). Cultured cortical neurons were transfected at 3-5 days *in vitro* (DIV) after initial plating onto glass chamber slides. For each chamber, 1-3 μg of pAAV-IRES-hrGFP containing either the FLAG-M_1 or FLAG-M_2 insert was mixed into 25 μL of a 0.25M solution of $CaCl_2$. This DNA solution was then mixed with 25 uL of a 2X HEPES solution (280mM NaCl, 50mM HEPES, 5 μM NaH_2PO_4, 10 μM Na_2HPO_4, pH 7.05) dropwise, vortexing between adding every few drops. The 50 μL mixture was then incubated at room temperature for 20 min and then added dropwise into the neuron culture medium and incubated in 5% CO_2 at 37°C for 1-3 hrs or overnight. Before incubation was over, fresh Neurobasal A Growth Medium (NBA-GM, see above) was pre-incubated in 10% at 37°C for 10-15 min. To terminate the transfection, the culture media containing the transfection mixture was removed from each chamber and replaced with the pre-incubated NBA-GM. The neurons were incubated for another 24 hrs. Neurons were washed twice with 1X PBS and then fixed with a paraformaldehyde solution (4% w/v paraformaldehyde, 4% w/v sucrose in 1X PBS) for 20-30 min at room temperature. After fixing, neurons were washed twice with 1X PBS. Chambers were removed from the slides, and slides were mounted using one drop of Vectashield mounting media (Vector Labs) per chamber surface, a coverslip placed on top of each chamber surface, and sealed with nail polish.

Lipofectamine Transfection of Primary Cortical Neurons - Transfection was performed on cultured cortical neurons using the primary culture technique described above. This protocol has been described previously by Gu and colleagues (2011). Cultured cortical neurons were transfected at 3-5 days *in vitro* (DIV) after initial plating onto glass chamber slides. For each chamber, 1-3 μg of pAAV-IRES-hrGFP containing either the FLAG-M_1 or FLAG-M_2 insert was diluted with OPTI-MEM (Gibco) to a volume of 500 μL. This DNA solution was mixed with a 500 μL solution of OPTI-MEM containing 1.6-4 μL of Lipofectamine reagent (Invitrogen) to final DNA(μg):Lipofectamine(μL) ratios of 1:1, 1:2, 1:2.5, and 1:5. The transfection mixtures were incubated at room temperature for 20 min. The cell culture media was aspirated from each chamber and replaced with 1mL of transfection mixture. Neurons were incubated for 20 min in 5% CO_2 at 37°C. Following incubation, the transfection media was aspirated out of each chamber and replaced with fresh NBA-GM (without penicillin and streptomycin). The neurons were then incubated in 5% CO_2 at 37°C for 40-48 hrs. Neurons were washed twice with 1X PBS and then fixed with a paraformaldehyde solution (4% w/v paraformaldehyde, 4% w/v sucrose in 1X PBS) for 20-30 min at room temperature. After fixing, neurons were washed twice with 1X PBS. Chambers were removed from the slides, and slides were mounted using one drop of Vectashield mounting media (Vector Labs) per chamber surface, a coverslip placed on top of each chamber surface, and sealed with nail polish.

Concentration and Titer of Recovered AAV stock solutions - AAV stocks containing the FLAG-M_1 and FLAG-M_2 were recovered from long-term storage at -80°C. Stocks were prepared previously by Dan Messinger according to calcium phosphate protocol (i) described above. Four 50 μL stocks of each AAV-M_1 or AAV-M_2 were concentrated by applying stocks to Millipore Centricon Plus-20 NMWL centrifugal filters and following procedures as outlined by the manufacture. The viral titer was determined in HT1080 cells using methods described above.

Transduction of Recombinant AAV - Primary cortical neurons were infected with AAV-M_1 at a MOI of 7.4x10-2, with AAV-M_2 at a MOI of $3.06x10^{-2}$ and with AAV-M_2 (MOI is expressed as infectious viral particles/neuron), or with a mock solution of ddH_2O at 3-5 DIV. Neurons were further incubated in 5% CO_2 at 37°C for 4-6 additional days. Neurons were washed twice with 1X PBS and then fixed with a paraformaldehyde solution (4% w/v paraformaldehyde, 4% w/v sucrose in 1X PBS) for 20-30 min at room temperature. After fixing, cells were washed once with PBS and then permeabilized by washing twice for 5 mins each with PBST (PBS with 0.2% Triton X-100). Cells were blocked for one hour at room temperature in blocking buffer (10% goat serum, 0.1M glycine, 0.05% sodium azide, 2% BSA). Blocking buffer was aspirated, and cells were incubated overnight at 4°C, shaking gently in anti-FLAG monoclonal antibody (Sigma-Aldrich) with either anti-MAP2 polyclonal antibody (Sigma-Aldrich) or moust anti-Tau1 monoclonal antibody (Millipore) diluted in blocking buffer. The next day, the primary antibody solution was removed, and each chamber was washed 3-4 times with PBST. Cells were incubated at room temperature for 3hrs with fluorescent secondary antibodies - goat anti-rabbit IgG conjugated to Alexa568 fluorophores and goat anti-mouse IgG conjugated to Alexa647 fluorophores. Cells were washed twice with PBST. Chambers were removed, and slides were mounted using one drop of Vectashield mounting media (Vector Labs) per chamber surface, a coverslip placed on top of each chamber surface, and sealed with nail polish.

Results

Immunocytochemistry Analysis of MAP2 and Tau1 - To visualize the somatodendritic and axonal domains of culture neurons, we fluorescently stained the somatodendritic marker MAP2 and axonal marker Tau1 with antibodies conjugated to Alexa 488 and Alexa 568 fluorophores, respectively. Complete polarization of neurons occurred around 6 days *in vitro* (DIV), where there was adequate separation between the green fluorescence of Alexa 488 and the red fluorescence of Alexa 568. (Fig 1.)

A MAP2 Tau1 Overlay

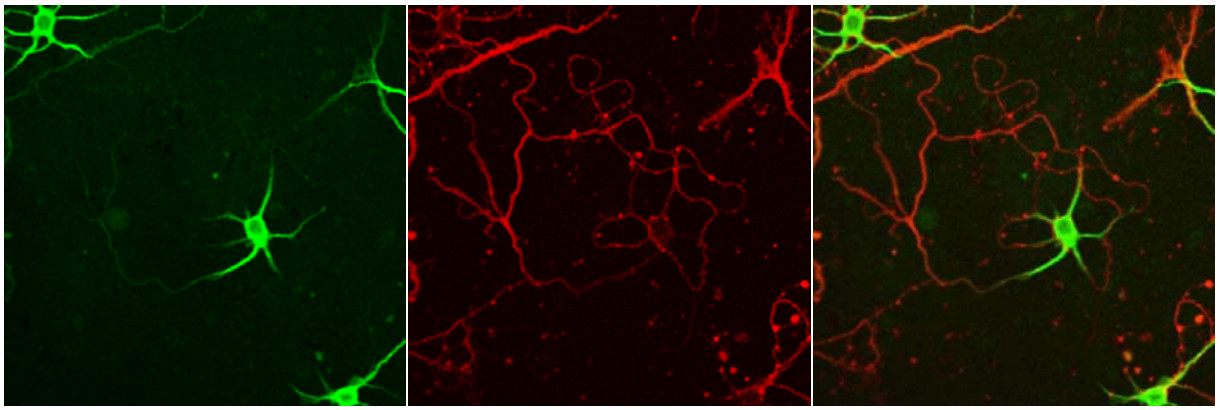

B

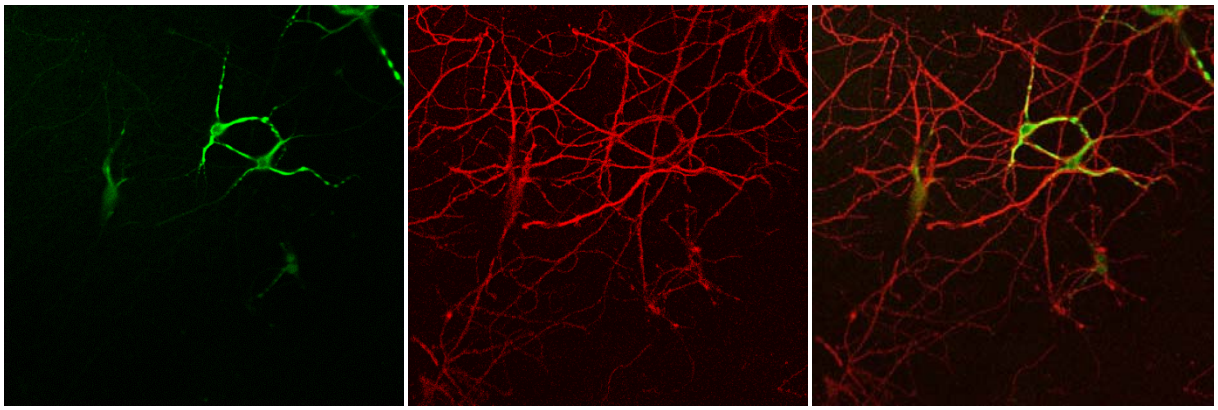

Figure 1. MAP2 and Tau1 fluorescent labeling in primary cortical neurons. Primary cortical neurons were stained for somatodendritic marker MAP2 (green) and axonal marker Tau1 (red). Sufficient polarization occurs by 8 days *in vitro* (B) and as early as 5 days *in vitro* (A), with separated green and red fluorescence.

Adeno-Associated Virus Production and Titer - To express the FLAG-tagged M_1 and M_2 receptors in neurons, we utilize adeno-associated viral (AAV) vectors to transduce a bicistronic DNA plasmid containing one of the FLAG-tagged receptors and a soluble GFP. AAV production involves the co-transfection of three plasmids encoding the rep and cap genes (AAV-RC), the E2A, E4, and VA RNA genes (pHelper), and the bicistronic plasmid containing either the M_1 or M_2 receptor and the soluble GFP (pAAV-IRES-hrGFP-FLAG-$M_{1/2}$).

Viral stocks produced from both attempted calcium phosphate protocols did not produce any fluorescence when determining viral titer using HT1080 cells, suggesting that no infectious virus particles were produced. Because of this, we attempted two additional approaches to expressing the FLAG-M_1 and FLAG-M_2 receptors: infecting primary neurons with previously-made AAV-M1 and AAV-M2 virus stocks and direct transfection of primary neurons using both calcium phosphate and Lipofectamine reagent protocols.

Calcium Phosphate Transfection of Primary Cortical Neurons - Neurons were transfected using the pAAV-IRES-hrGFP plasmid containing either FLAG-M_1 or FLAG-M_2. Calcium phosphate transfection protocols seem to be toxic to cultured cells, with most cells dying within 5-7 days. Cells that survived showed no fluorescence above mock transfected controls when visualized with a confocal microscope.

Lipofectamine Transfection of Primary Cortical Neurons - Neurons were transfected using the pAAV-IRES-hrGFP plasmid containing either FLAG-M_1 or FLAG-M_2. Transfection protocol with Lipofectamine reagent seems to be toxic to cultured cells, with most cells dying within 4-6 days. Cells that survived showed no fluorescence above mock transfected controls when visualized with a confocal microscope.

Concentration and Titer of AAV stocks - 50 μL AAV virus stocks previously made by the lab and stored long term were thawed and concentrated 4-fold. Concentrated stocks of AAV-M_1 showed 36% ± 10%

infection rate using a 1/100 dilution; a 7.6% ± 6.4% infection rate using a 1/1000 dilution, and no infection using a 1/10000 dilution. The viral titer of AAV-M_1 was calculated to be $5.4x10^6 \pm 1.67x10^6$ virus/500uL. Concentrated stocks of AAV-M_2 showed a 15% ±4.1% infection rate using a 1/100 dilution and no infection using either a 1/1000 or 1/10000 dilution. The viral titer of AAV-M_2 was calculated to be $2.3x10^6 \pm 0.616x10^6$ virus/500uL.

AAV Transduction of Primary Cortical Neurons - Infected neurons did not show fluorescence above mock infected neurons.

Discussion

Many of the studies in neuronal polarity and subcellular localization of sorted proteins utilize one of two main *in vitro* model systems: rodent embryonic hippocampal pyramidal neurons (Kaech and Banker, 2006) or postnatal cerebellar granule neurons (Powell et al., 1997). One of the main advantages of using *in vitro* systems is the ability of dissociated neurons in culture to polarize into their morphologically and functionally distinct domains separate from the complexity of the nervous system. Also, biological manipulations can be more readily performed on neurons cultured *in vitro* (Tahirovic and Bradke, 2009). Here, we took advantage of an *in vitro* system to explore muscarinic receptor M_1 and M_2 localization in cortical neurons. Marked separation of somatodedritic marker MAP2 and axonal marker Tau1 within 7-8 DIV demonstrates the viability of the primary neuron culture system as a means for studying protein sorting to both domains. These domain markers also present a reliable means of defining the two neuronal domains when visualizing subcellular protein localization using immunofluorescence.

Further, immunofluorescence microscopy has been utilized successfully in the past to visualize subcellular localization of epitope-tagged mAChRs (Nadler and Nathanson, 2001; Chmelar and Nathanson, 2006). Here, we attempted to utilize the same approach to visualize the subcellular localization of FLAG-tagged M_1 and M_2 mAChRs in cortical neurons. Our first system attempted was the use of adeno-associated viral vectors (AAV) to express the FLAG-tagged receptors in primary neurons.

The AAV system presents two advantages. First, transduction of genes via AAV vectors allows for a more long-term expression of the genes of interest compared to transient expression via common transfection methods. This allows the gene of interest to be expressed more continuously throughout the 7-8 days that the neuronal polarization process takes to complete. Second, the expression of a soluble GFP allows for the quick identification infected neurons under a fluorescence microscope and also allows us to visualize the entire cytoplasmic volume of an infected neuron. We encountered difficulty in producing infectious AAV particles, with prepared viral stocks failing to confer soluble GFP expression into permissive HT1080 cells.

We then attempted to directly transfect primary neurons using both calcium phosphate and Lipofectamine reagent protocols for transient expression of the M_1 and M_2 receptors. Both calcium phosphate and Lipofectamine protocols were highly cytotoxic to infected neurons compared to their untransfected mock controls, with most transfected neurons dying within 4-6 days after transfection. Of the neurons that survived, none displayed fluorescence, suggesting that neither DNA was successfully delivered into the neurons. Given the nature of the mechanisms of calcium phosphate and lipofectamine transfection (namely the disruption of the plasma membrane) and the high sensitivity of primary neurons in culture, an alternative possibility could be that all neurons that were successfully transfected also became nonviable as a consequence of the transfection mechanism.

We finally tried using AAV-M_1 and AAV-M_2 stocks that had been previously prepared in the lab and stored at -80°C for several years. Anticipating that the viral titer (infectious viral particles per volume of stock solution) had diminished over the years, these stocks were concentrated 4-fold before attempting to use them experimentally. The viral titer that was determined for these concentrated stocks were still relatively low compared to what one would expect from a more recently-prepared viral stock. Attempts to visualize FLAG-tagged receptors in neurons infected with these stocks were unsuccessful. Neurons showed no fluorescence above mock infection controls, suggesting that infectious particles failed to infect the neurons or that all infected neurons did not remain on the glass slide following the

immunocytochemistry protocol. Another possibility could be the failure of the α-FLAG primary antibody to bind any expressed receptors.

Despite these attempts to express and visualize the FLAG- M_1 and FLAG-M_2 receptors in primary neurons, these experiments to illustrate M_1 and M_2 plasma membrane sorting in cortical neurons were inconclusive.

A possible alternative approach to exploring this question in future experiments would be immunofluorescence using subtype specific antibodies to the M_1 and M_2 receptors. This approach, however has one major caveat. mAChR subtype-specific antibodies that are suitable for immunoprecipitation and Western blots are usually not as specific when used in immunocytochemical analysis (Hamilton and Nathanson, unpublished).

Another approach could be exploring the interaction, if any, of mAChR subtypes and kinesin motor proteins that deliver vesicle cargo to specific neuronal subdomains. For example, in 7 DIV cultured hippocampal neurons, KIF-17 kinesin motor proteins shuttle vesicle cargo containing dedritic proteins such as the NMDA receptor subunit NR2B to dendrites, while KIF-5 motor proteins transport vesicle cargo contining axonal proteins such as VAMP2 to the presynaptic axon terminal (Song et al., 2009). Immunoprecipitation experiments can be used to pull down mAChR complexes from cortical tissue, and subsequent Western blot analysis using antibodies toward subdomain-specific KIF proteins can give us insight into not only the subcellular localization of mAChRs, but also the possible mechanism by which the receptor is sorted.

CHAPTER 3

Effects of Dimerization of the M_1 and M_2 Muscarinic Acetylcholine Receptors in Madin-Darby Canine Kidney Cells

Introduction

The phenomenon of GPCR dimerization has been studied for decades. Numerous studies provide evidence that GPCRs form functional dimers and possibly higher order oligomers (Breitwieser, 2004). GPCR dimerization has implications on receptor-ligand binding, activation, signaling, and receptor trafficking (Breitwieser, 2004).

Early evidence for mAChR dimerization and oligomerization involved complex binding curves of mAChR agonists and antagonists which suggested multiple affinity states and therefore binding sites located on dimeric receptors (Hirschberg and Schimerilik, 1994; Potter et al., 1991). Other studies used α_2-adrenergic/M_3 muscarinic receptor chimeras consisting of the first 5 transmembrane domains (TMD) of one receptor and the last 2 TMDs of the other. Ligand binding and activity were not seen in either chimera expressed alone, but binding and activity were present when the receptors were co-expressed, suggesting an intermolecular interaction between two null receptors that are then functional upon dimerization (Maggio et al., 1993).

More recent bioluminescence resonance energy transfer (BRET) experiments provided further evidence of mAChR dimerization. The M_1, M_2, and M_3 mAChRs were fused with either the energy donor *Renilla* luciferase (*R*Luc) or the energy accepting yellow fluorescence protein (YFP). Varied combinations of these fusion proteins were coexpressed in JEG-3 cells or HEK293 cells. BRET data obtained from these studies demonstrate that the M_1, M_2, and M_3 mAChRs can each homdimerize with itself and heterodimerize with each other (Goin and Nathanson, 2006).

In this study, we explore the influence of receptor dimerization on the plasma membrane sorting of mAChRs. Given that the apically sorted M_2 receptor can heterodimerize with either of the basolaterally sorted M_1 and M_3 receptors (Nadler et al., 2001; Chmelar and Nathanson, 2006; Goin and Nathanson, 2006), we wanted to know how the plasma membrane sorting of the M_2 receptor and its $M_{1/3}$ partner

would be affected by their dimerization in MDCK II cells. We expect one of two scenarios to occur: either the apically sorted M_2 receptor will change to basolateral sorting with its $M_{1/3}$ dimer partner, or the basolaterally sorted $M_{1/3}$ receptor will change to apical sorting with its M_2 dimer partner. To answer this question we co-transfected MDCK II cells with a FLAG-tagged M_2 and a HA-tagged M_1 or HA-tagged M_3 receptor. We utilized immunfluorescence staining to visualize any changes in membrane sorting.

Experimental Procedures

Fluorescence Microscopy - Fluorescent images were collected using a Nikon Eclipse E600 microscope (Nikon Co.) using 40X dry lens at the Keck Microscopy Facility at the University of Washington.

Cell Culture – MDCK II cell lines were previously obtained from Dr. Keith Mostov (University of California, San Francisco). Cell lines were maintained in Dulbecco's modified Eagle's medium (DMEM) supplemented with 10% fetal bovine serum, 100 units/mL penicillin G and 0.1mg/mL streptomycin sulfate. Cells were incubated in a humidified 10% CO_2 environment at 37°C.

DNA Plasmid Constructs - The cloned HA-tagged M_1 and M_3 receptors were obtained from the UMR cDNA Resource Center. The human M_1 muscarinic acetylcholine receptor has an N-terminal 3X humagglutinin tag and was cloned into pcDNA3.1+ (Invitrogen) using the 5' KpnI and 3' XhoI restriction sites. The human M_3 muscarinic acetylcholine receptor has an N-terminal 3X humagglutinin tag and was cloned into pcDNA3.1+ (Invitrogen) using the 5' KpnI and 3' XbaI restriction sites.

The FLAG-M_2 receptor was first constructed as described previously by Nadler et al. (2001). Briefly, porcine M_2 was cloned into the mammalian expression vector using PCR with primers coding for select restriction sites to flank the receptor coding sequences. A modified FLAG epitope was added to the extracellular N-terminal immediately following the initiator methionine. Two different FLAG-tagged M_2 constructs were used in this study. The first FLAG-M_2 DNA construct was cloned into the pCDPS

expression vector previously by Nadler et al. (2001). The second FLAG-M_2 DNA construct was cloned into the pcDNA3.1+ DNA vector previously by Cindy Reiner.

Calcium Phosphate Transfection of MDCK II cells – MDCK II cells were plated on 2-well glass chamber slides (Thermo Scientific) and incubated in cell culture conditions (described above) until fully confluent. There were four transfection conditons: untransfected mock, HA-$M_{1/3}$ alone, FLAG-M_2 alone, and both HA-$M_{1/3}$ and FLAG- M_2 together. For each chamber of a single-plasmid transfection, 2 µg of DNA were used. For each chamber of a two-plasmid transfection, 2 µg of each DNA were used. For each chamber, the DNA was mixed into 25 µL of a 0.25M solution of $CaCl_2$. This DNA solution was then mixed with 25 uL of a 2X HEPES solution (280mM NaCl, 50mM HEPES, 5 µM NaH_2PO_4, 10 µM Na_2HPO_4, pH 7.05) dropwise, vortexing between adding every few drops. The 50 µL mixture was then incubated at room temperature for 20 min and then added dropwise into the cell culture medium and incubated overnight. The following morning, the culture medium was replaced with fresh DMEM containing no supplements. The cultures were then incubated for another 48 hours before fixing.

Immunocytochemistry Analysis of HA-$M_{1/3}$ and FLAG-M_2 - Cell culture media was aspirated from each chamber and washed twice with phosphate buffered saline (PBS) (0.8% NaCl, 0.02% KCl, 0.12% Na_2HPO_4, 0.02% KH_2O_4, 0.01% $MgCl_2$, 0.01% $CaCl_2$, pH 7.4). Cells were then fixed with 4% PFA in PBS at room temperature for 20-30 min. Cells were washed once with PBS and then permeabilized by washing twice for 5 mins with PBST (PBS with 0.2% Triton X-100). Cells were blocked for one hour at room temperature in blocking buffer (10% goat serum, 0.1M glycine, 0.05% sodium azide, 2% BSA). Blocking buffer was aspirated, and cells were incubated overnight at 4°C, shaking gently in mouse anti-FLAG M2 monoclonal antibody (Sigma-Aldrich) diluted to 1.2µg/mL in blocking buffer. The next day, the first primary antibody solution was removed, and each chamber was washed 3-4 times with PBST. Cell were then incubated again overnight at 4°C, shaking gently in rabbit anti-HA polyclonal antibody diluted 1/500 in blocking buffer. The next day, the second primary antibody solution was removed, and

each chamber was washed 3-4 times with PBST. Cells were incubated at room temperature for 3hrs with fluorescent secondary antibodies - goat anti-rabbit IgG conjugated to Alexa488 fluorophores and goat anti-mouse IgG conjugated to Alexa568 fluorophores. Cells were washed twice with PBST. Chambers were removed, and slides were mounted using one drop of Vectashield mounting media (Vector Labs) per chamber surface, a coverslip placed on top of each chamber surface, and sealed with nail polish. For non-permeablized conditions, the permeabilization step was omitted, and all steps and solutions using PBST used 1X PBS instead.

Results

Calcium Phosphate Transfection and Immunocytochemistry of MDCK II cells - Calcium phosphate transfection protocol was performed and immunocytochemical analysis was performed using both permeabilized and non-permeabilized conditions. Transfection of HA-M_1 alone showed localization of M_1 receptors to both the basolateral and apical plasma membranes in permeabilized conditions. Transfection of FLAG-M_2 alone and FLAG-M_2 with HA-M_1 showed no fluorescence above untransfected controls. No fluorescence above untransfected controls was observed for all transfection conditions stained in non-permeabilized conditions.

Discussion

Dimerization has implications on many aspects of GPCR function such as ligand affinity, signaling, and receptor trafficking. Indeed, some receptors require dimerization in for proper subcellular localization. Dimerization of the $GABA_{B1}$ and $GABA_{B2}$ receptors masks ER retention signals so that the receptors can continue on to the plasma membrane (Calver et al., 2001; Pagano et al., 2001). Homodimerization of β_2-adrenergic receptors are required for ER export and trafficking to the membrane (Salahpour et al., 2004). Here, we use a classic biological model for epithelial cell polarity, MDCK cells, to study the role of dimerization if any on membrane sorting of mAChR.

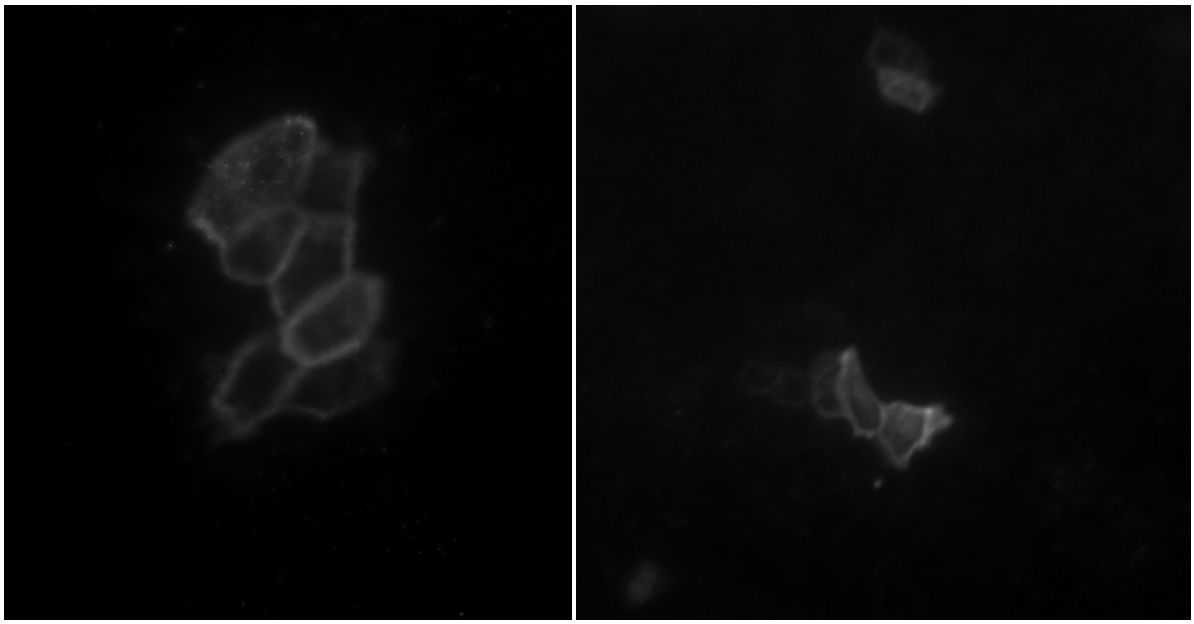

Figure 2. HA-M_1 fluorescent labeling in MDCK II under permeabilized conditions. MDCK II cells were transiently transfected with HA-tagged M_1 receptors and fluorescently stained for the HA tag. Fluorescent staining shows the M_1 receptor localized primarily basolaterally (left) but some images show fluorescence that could correspond to apically sorted or intracellular receptors.

The non-preferential sorting of the HA-M_1 receptor seen in the fluorescent staining under permeabilized conditions is consistent with similar results seen by Nadler et al. (2001) using a FLAG-tagged M_1 receptor transiently expressed in MDCK II cells. However, Shmuel et al. (2007) show that the M1 receptor is sorted basolaterally in immunocytochemical analysis under non-permeabilized conditions.

The lack of fluorescence in MDCK II cells transfected with FLAG-M_2 alone or co-transfected with FLAG-M_2 and HA-M_1 suggests that the MDCK II cells did not successfully take up the transfection DNA. Another possibility is that the anti-FLAG antibody failed to bind to the expressed FLAG-M_2 receptors. Though, this would not fully explain the lack of fluorescence in the co-transfection because the anti-HA antibody successfully stained the MDCK II cells transfected with the HA-M_1 receptor alon. The lack of fluorescence in MDCK II cells transfected with HA-M_1 alone and stained under non-permeabilized conditions but not permeabilized conditions suggests that the MDCK II cells failed to take up the transfection DNA.

These experiments to determine the role, if any, of dimerization on mAChR membrane sorting were inconclusive. However, given that the M_2 receptor arrives at the apical membrane via transcytosis from the basolateral membrane, and that apical sorting signals tend to act recessively in the presence of more dominant basolateral sorting signals (Chmelar and Nathanson, 2006), we predict that a dimer consisting of M_2 and $M_{1/3}$ would localize to the basolateral membrane. Future work on this project would include optimization of the calcium phosphate transfection protocol. Also, other transfection protocols such as Lipofectamine reagent protocols could be utilized.

Conclusions

Proper sorting and trafficking of membrane proteins in polarized cells is crucial to cellular function. The experiments described in this thesis were intended to investigate a few aspects of muscarinic receptor membrane sorting: the membrane sorting of the M_1 and M_2 receptors in cortical neurons and the role of dimerization in plasma membrane sorting.

Preliminary fluorescence data suggested that the M_1 receptor is sorted somatodendritcally in cortical neurons, while the M_2 receptor was not preferentially sorted to either the somatodendritic or axonal domains. The data, however, lacked somatodendritic and axonal markers. Primary cortical neuron cultures are shown here to be a suitable *in vitro* model for studying neuronal polarity when fluorescently stained for MAP2 and Tau1. Polarization of cultured cortical neurons seems to occur by 5-7 days *in vitro*. The membrane sorting of M_1 and M_2 receptors in cortical neurons remains inconclusive.

Previous work has shown that the apically-sorted M_2 receptor can dimerize with both the basolaterally-sorted M_1 and M_3 receptors. We intended to explore how plasma membrane sorting of two differentially-sorted receptors would be affected when they are dimerized. We confirm here that an epitope-tagged M_1 receptor is localized mostly basolaterally when transiently expressed in MDCK II cells, consistent with results from previous studies. Because transient expression of epitope-tagged M_2 receptors and co-expression of epitope-tagged M_1 and M_2 receptors were not successful, the role of dimerization in plasma membrane sorting of muscarinic receptors remains inconclusive.

References

1. Arimura N. and Kaibuchi K. (2005). “Key regulators in neuronal polarity.” *Neuron*. **48**:881-884.
2. Bacallao R.L., McNeill H. (2009). "Cystic kidney diseases and planar cell polarity signaling." *Clin. Genet.* **75**:107-117.
3. Barnes A.P. and Polleux F. (2009). “Establishment of Axon-Dendrite Polarity in Developing Neurons.” *Annu. Rev. Neurosci.* **32**:347-381.
4. Bermak J.C., Li M., Bullock C., and Zhou Q. (2001). "Regulation of transport of the dopamine D1 receptor by a new membrane-associated ER protein." *Nat. Cell Biol.* **3**:492-498.
5. Bernard V., Levey A.I., and Bloch B. (1999). "Regulation of the subcellular distribution of m4 muscarinic acetylcholine receptors in striatal neurons in vivo by the cholinergic environment: evidence for regulation of cell surface receptors by endogenous and exogenous stimulation." *J. Neurosci.* **19**:10237-10249.
6. Bonifacino J.S. and Traub L.M. (2003). "Signals for sorting of transmembrane proteins to endosomes and lysosomes." *Annu. Rev. Biochem.* **72**:395-447.
7. Bradke F. and Dotti C.G. (1997). “The role of local actin instability in axon formation.” *Science.* **283**:1931-1934.
8. Breitwieser G.E. (2004). "G protein-coupled receptor oligomerization: implications for G protein activation and cell signaling." *Circ. Res.* **94**:17-27.
9. Brown P.S., Wang E., Aroeti B., Chapin S.J., Mostov K.E., Dunn K.W. (2000). "Definition of distinct compartments in polarized Madin-Darby canine kidney (MDCK) cells for membrane-volume sorting, polarized sorting and apical recycling." *Traffic*. **1**:124-140.
10. Burridge K. and Wennerberg K. (2004). “Rho and Rac take center stage.” *Cell*. **116**:167-179.
11. Caceres A. and Kosik K.S. (1990). “Inhibition of neurite polarity by tau antisense oligonucleotides in primary cerebellar neurons.” *Nature*. **343**:461-463.

12. Caceres A., Mautino J., and Kosik K.S. (1992). “Suppression of MAP2 in cultured cerebellar macroneurons inhibits minor neurite formation.” *Neuron*. **9**:607-618.

13. Calver A.R., Robbins M.J., Cosio C., Rice S.Q., Babbs A.J., Hirst W.D., Boyfield I., Wood M.D., Russell R.B., Price G.W., Couve A., Moss S.J., and Pangalos M.N. (2001). "The C-terminal domains of the GABA(b) receptor subunits mediate intracellular trafficking but are not required for receptor signaling." *J. Neurosci*. **21**:1203-1210.

14. Cao X., Surma M.A., Simons K. (2012). "Polarized sorting and trafficking in epithelial cells." *Cell Research* **22**:793-805.

15. Carmosino M., Rizzo F., Procino G., Basco D., Valenti G., Forbush B., Schaeren-Wiemers N., Caplan M.J., Svelto M. (2010). “MAL/VIP17, a new player in the regulation of NKCC2 in the kidney.” *Mol. Biol. Cell.* **21(22)**:3985-97.

16. Casanova J.E., Apodaca G., Mostov K.E. (1991). "An autonomous signal for basolateral sorting in the cytoplasmic domain of the polymeric immunoglobulin receptor." *Cell*. **66(1)**:65-75.

17. Caulfield M.P., Birdsall N.J.M. (1998). "International Union of Pharmacology. XVII. Classification of Muscarinic Acetylcholine Receptors." *Pharmacol. Rev.* **50(2)**:279-90.

18. Chicka M.C. and Strethler E.E. (2003). “Alternative splicing of the first intracellular loop of plasma membrane Ca2+-ATPase isoform 2 alters its membrane targeting.” *J. Biol. Chem.* **278(20)**:18464-70.

19. Chmelar R.S., and Nathanson N.M. (2006). “Identification of a novel apical sorting motif and mechanism of targeting of the M2 muscarinic acetylcholine receptor.” *J. Biol. Chem*. **281**:35381-35396.

20. Chuang J.Z. and Sung C.H. (1998). “The cytoplasmic tail of rhodopsin acts as a novel apical sorting signal in polarized MDCK cells.” *J. Cell Biol.* **142**:1245-1256.

21. Da Silva J.S., Hasegawa T., Miyagi T., Dotti C.G., Abad-Rodriguez J. (2005). “Asymmetric membrane ganglioside sialidase activity specifies axonal fate.” *Nat. Neurosci*. **8**:606-615.

22. Datta A., Bryant D.M., Mostov K.E. (2011). "Molecular Regulation of Lumen Morphogenesis." *Current Biology*. **21:**R126-136.

23. de Forges H., Bouissou A., Perez F. (2012). "Interplay between microtubule dynamics and intracellular organization." *Internat. J. Biochem. Cell Biol.* **44**:266-274.

24. Dudek H., Ghosh A., and Greenberg M.E. (2001). "Calcium phosphate transfection of DNA into neurons in primary culture." *Curr. Protoc. Neurosci*. Chapter 3:Unit3.11.

25. Erisir A., Levey A.I., and Aoki C. (2001). "Muscarinic receptor M(2) in cat visual cortex: Laminar distribution, relationship to gamma-aminbutyric acidergic neurons, and effect of cingulate lesions." *J. Comp. Neurol*. **441**:168-185.

26. Fiedler K., Simons K. (1995). "The role of N-gylcans in the secretory pathway." *Cell.* **81**:309-312.

27. Folsch H., Mattila P.E., Weisz O.A. (2009). "Taking the scenic route: biosynthetic traffic to the plasma membrane in polarized epithelial cells." *Traffic.* **10**:972-981.

28. Fukata Y., Itoh T.J., Kimura T., Menager C., Nishimura T., Shiromizu T., Watanabe H., Inagaki N., Iwamatsu A., Hotani H., et al. (2002). "CRMP-2 binds to tubulin heterodimers to promote microtubule assembly." *Nat. Cell Biol.* **4**:583-591.

29. Garvalov B.K., Flynn K.C., Neukirchen D., Meyn L., Teusch N., Wu X., Brakebusch C., Bamburg J.R., and Bradke F. (2007). "Cdc42 regulates cofilin during the establishment of neuronal polarity." *J. Neurosci*. **27**:13117-13129.

30. Goin J.C. and Nathanson N.M. (2006). "Quantitative Analysis of the Muscarinic Acetylcholine Receptor Homo- and Heterodimerization in Live Cells." *J. Biol. Chem.* **281**:5416-5425.

31. Grubb M.S. and Burrone J. (2010). "Building and maintaining the axon initial segment." *Curr. Opin. Neurobiol.* **20**:481-488.

32. Gu Y., Barry J., McDougel R., Terman D., and Gu C. (2012). "Alternative splicing regulates kv3.1 polarized targeting to adjust maximal spiking frequency." *J. Biol. Chem.* **287**:1755-1769.

33. Hannan L.A., Lisanti M.P., Rodriguez-Boulan E., Edinin M. (1993). “Correctly sorted molecules of GPI-anchored protein are clustered and immobile when they arrive at the apical surface of MDCK cells.” *J. Cell Biol.* **120**:353-358.

34. Heasman S.J. and Ridley A.J. (2008). “Mammalian Rho GTPases: New insights into their functions from *in vivo* studies.” *Nat. Rev. Mol. Cell Biol.* **9**:690-701.

35. Hedstrom K.L, Xu X., Ogawa Y., Frischknecht R., Seidenbecher C.I., Shrager P., and Rasband M.N. (2007). “Neurofascin assembles a specialized extracellular matrix at the axon initial segment.” *J. Cell Biol.* **178**:875-886.

36. Hedstrom K.L., Ogawa Y., and Rasband M.N. (2008). "AnkyrinG is required for maintenance of the axon initial segment and neuronal polarity." *J. Cell Biol.* **183**:635-640.

37. Hirschberg B.T. and Schimerlik M.I. (1994). "A kinetic model for oxotremorine M binding to recombinant porcine m2 muscarinic receptors expressed in Chinese hamster ovary cells." *J. Biol. Chem.* **269**:26127-26135.

38. Hunziker W. and Fumey C. (1994). "A di-leucine motif mediates endocytosis and basolateral sorting of macrophage IgG Fc receptors in MDCK cells." *EMBO J.* **13(13)**:2963-9.

39. Inagaki N., Chihara K., Arimura N., Menager C., Kawano Y., Matsuo N., Nishimura T., Amano M., and Kaibuchi K. (2001). “CRMP-2 induces axons in cultured hippocampal neurons.” *Nat. Neurosci*. **4**:781-782.

40. Iverson H.A., Fox D., Nadler S., Klevit, R.E., and Nathanson N.M. (2005). "Identification and Structural Determination of the M3 Basolateral Sorting Signal." *J. Biol. Chem.* **280**:24568-24575.

41. Jacobs T., Causeret F., Nishimura Y.V., Terao M., Norman A., Hoshino M., and Nikloic M. (2007). “Localized activation of p21-activated kinase controls neuronal polarity and morphology.” *J. Neurosci.* **27**:8604-8615.

42. Jaffe A.B. and Hall A. (2005). “Rho GTPases: Biochemistry and biology. *Annu. Rev. Cell Dev. Biol.* **21**:247-269.

43. Kaech S. and Banker G. (2006). “Culturing hippocampal neurons.” *Nat. Protoc.* **1**:2406-2415.

44. Kaupman K., Malitschek B., Schuler V., Heid J., Froestl W., Beck P., Mosbacher J., Bischoff S., Kulik A., Shigemoto R., Karschin A., and Bettler B. (1998). "$GABA_B$-receptor subtypes assemble into functional heteromeric complexes." *Nature*. **396**:683-687.

45. Kawano Y., Yoshimura T., Tsuboi D., Kawabata S., Kaneko-Kawano T., Shirataki H., Takenawa T., and Kaubuchi K. (2005). "CRMP-2 is involved in kinesin-1-dependent transport of the Sra-1/WAVE complex and axon formation." *Mol. Cell Biol.* **25**:9920-9935.

46. Kinoshita T., Fujita M., Maeda Y. (2008). "Biosynthesis, remodeling and functions of mammalian GPI-anchored proteins: recent progress." *J. Biochem.* **144**:287-294.

47. Klein W.L., Nathanson N., and Nirenberg M. (1979). "Muscarinic acetylcholine receptor regulation by accelerated rate of receptor loss." *Biochem. Biophys. Res. Comm.* **90**:506-512.

48. Klemm R.W., Ejsing C.S., Surma M.A., Kaiser H.J., Gerl M.J., Sampaio J.L., de Robbilard Q., Ferguson C., Proszynski T.J., Shevchenko A., Simons K. (2009). "Segregation of sphingolipids and sterols during formation of secretory vesicles at the trans-Golgi network." *J. Cell Biol.* **185(4)**:601-12.

49. Kobayashi T., Storrie B., Simons K., and Dotti C.G. (1992). "A functional barrier to movement of lipids in polarized neurons." *Nature.* **359**:647-650.

50. Koh C.G. (2006). "Rho GTPases and their regulators in neuronal functions and development." *Neurosignals*. **15**:228-237.

51. Koivisto U.M., Hubbard A.L., Mellman I. (2001). "A novel cellular phenotype for familial hypercholesterolemia due to a defect in polarized targeting of LDL receptor." *Cell*. **105(5)**:575-85.

52. Kole M.H., Ilschner S.U., Kampa B.M., Williams S.R., Ruben P.C., and Stuart G.J. (2008). "Action potential generation requires a high sodium channel density in the axon initial segment." *Nat. Neurosci.* **11**:178-186.

53. Krause M., Dent E.W., Bear J.E., Loureiro J.J., and Gertler F.B. (2003). "Ena/VASP proteins: regulators of the actin cytoskeleton and cell migration." *Annu. Rev. Cell Dev. Biol.* **19**:541-564.

54. Krause M., Leslie J.D., Stewart M., Lafuente E.M., Valderrama F., Jagannathan R., Strasser G.A., Rubinson D.A., Liu H., Way M., et al. (2004). “Lamellipodin, an Ena/VASP ligand, is implicated in the regulation of lamellipodial dynamics.” *Dev. Cell* **7:**571-583.

55. Lacas-Gervais S., Guo J., Strenzke N., Scarfone E., Kolpe M., Jahkel M., De Camilli P., Moser T., and Rasband M.N. (2004). “BetaIVSigma1 spectrin stabilizes the nodes of Ranvier and axon initial segments.” *J. Cell Biol.* **166**:983-990.

56. Levey A.I., Edmunds S.M., Koliatsos W., Wiley R.G., and Heilman C.J. (1995). "Expression of m1-m4 muscarinic acetylcholine receptor proteins in rat hippocampus and regulation by cholinergic innervation." *J. Neurosci*. **15**:4077-92.

57. Levey A.I., Kitt C.A., Simonds W.F., Price D.L., and Brann M.R. (1991). "Identification and localization of muscarinic acetylcholine receptor proteins in brain with subtype-specific antibodies." *J. Neurosci*. **11**:3218-26.

58. Li Q., Luo X., Muallem S. (2004). "Functional mapping of Ca2+ signaling complexes in plasma membrane microdomains of polarized cells." *J. Biol. Chem.* **279**:27837-278340.

59. Li R. and Gundersen G.G. (2008). “Beyond polymer polarity: How the cytoskeleton builds a polarized cell.” *Nat. Rev. Mol. Cell Biol.* **9**:860-73.

60. Lisanti M.P., Caras I.W., Davitz M.A., Rodriguez-Boulan E. (1989). “A glycophospholipid membrane anchor acts as an apical targeting signal in polarized epithelial cells.” *J. Cell Biol.* **109(5)**:2145-56.

61. Lisanti M.P., Sargiacomo M., Graeve L., Saltiel A.R., Rodriguez-Boulan E. (1989). “Polarized apical distribution of glycosyl-phosphotidylinosital-anchored proteins in a renal epithelial cell line.” *Proc. Natl. Acad. Sci. USA.* **85**:9557-9561.

62. Madziva M.T. and Birnbaumer M. (2006). "A Role for ADP-ribosylation Factor 6 in the Processing of G-protein-coupled Receptors." *J. Biol. Chem.* **281**:12178-12186.

63. Maggio R., Vogel Z., and Wess J. (1993) "Coexpression studies with mutant muscarinic/adrenergic receptors provide evidence for intermolecular "cross-talk" between G-protein-linked receptors." *Proc. Natl. Acad. Sci. USA.* **90**:3103-3107.

64. Matus-Leibovitch N., Lupu-Meiri M., and Oron Y. (1990). "Two types of intrinsic muscarinic responses in Xenopus oocytes. II. Hemispheric asymmetry of responses and receptor distribution." *Pflugers. Archiv.* **417**:194-199.

65. Mellman I., Nelson J. (2008). "Coordinated protein sorting, targeting and distribution in polarized cells." *Nat. Rev. Mol. Cell Biol.* **9(11)**:833-45.

66. Mohler P.J., Schott J., Gramolini A.O., Dilly K.W., Guatimosim S., duBell W.H., Song L., Huarogné K., Kyndt F., Ali M.E., Rogers T.B., Ledere W.J., Escande D., Le Marec H., Bennet V. (2003). "Ankryin-B mutation causes type 4 long-QT arrhythmia and sudden cardiac death." *Nature.* **421**:536-639.

67. Mostov K.E., de Bruyn Kops A., Deitcher D.L. (1986). "Deletion of the cytoplasmic domain of the polymeric immunoglobulin receptor prevents basolateral localization and endocytosis." *Cell.* **47(3)**:359-64.

68. Nadler L.S., Kumar G., and Nathanson N.M. (2001). "Identification of a basolateral sorting signal for the M3 muscarinic acetylcholine receptor in Madin-Darby canine kidney cells." *J. Biol. Chem.* **276**:10539-10547.

69. Naesens M., Steels P., Verberckmoes R., Vanrenterghem Y., Kuypers D. (2004). "Bartter's and Gitelman's syndromes: from gene to clinic." *Nephron Physiol.* **96:**65-78.

70. Nakada C., Ritchie K., Oba Y., Nakamura M., Hotta Y., Iino R., Kasai R.S., Yamaguchi K., Fujiwara T., and Kusumi A. (2003). "Accumulation of anchored proteins forms membrane diffusion barriers during neuronal polarization." *Nat. Cell Biol.* **5**:626-632.

71. Nathanson N.M. (2008). "Synthesis, Trafficking, and Localization of Muscarinic Acetylcholine Receptors." *Pharmacol. Ther.* **119(1)**:33-43.

72. Ng J. and Luo L. (2004). “Rho GTPases regulate axon growth through convergent and divergent signaling pathways.” *Neuron*. **44**:779-793.

73. Nishimura K., Akiyama H., Komada M., and Kamiguchi H. (2007). " βIV-spectrin forms a barrier against L1CAM at the axon initial segment." *Mol. cell Neurosci.* **34**:422-430.

74. Ogawa Y. and Rasband M.N. (2008). “The functional organization and assembly of the axon initial segment.” *Curr. Opin. Neurobiol.* **18**:307-313.

75. Pagano A., Rovelli G., Mosbacher J., Lohmann T., Duthey B., Stauffer D., Ristig D., Schuler V., Meigel I., Lampert C., Stein T., Prezeau L., Blahos J., Pin J., Proestl W., Kuhn R., Heid J., Kaupmann K., and Bettler B. (2001). "C-terminal interaction is essential for surface trafficking but not for heteromeric assembly of GABA(b) receptors." *J. Neurosci*. **21**:1189-1202.

76. Paladino S., Lebreton S., Tivodar S., Campana V., Tempre R., Zurzolo C. (2008). “Different GPI-attachment signals affect that oligomerisation of GPI-anchored proteins and their apical sorting.” *J. Cell Sci.* **121**:4001-4007.

77. Palay S.L., Sotelo C., Peters A., and Orkand P.M. (1968). "The axon hillock and the initial segment." *J. Cell Biol*. **38**:193-201.

78. Parkinson N.J., Olsson C.L., Hallows J.L., McKee-Johnson J., Keogh B.P., Noben-Trauth K., Kujawa S.G., and Tempel B.L. (2001). “Mutant beta-spectrin 4 causes auditory and motor neuropathies in quivering mice.” *Nat. Genet.* **26**:61-65.

79. Phaffinger P.J., Martin J.M., Hunter D.D., Nathanson N.M., Hille B. (1985). "GTP-binding proteins couple cardiac muscarinic receptors to a K channel." *Nature.* **317(6037)**:563-8.

80. Potter L.T., Ballesteros L.A., Bichajian L.H., Ferrendelli C.A., Fisher A., Hanchett H.E., and Zhang R. (1991). "Evidence of paired M2 muscarinic receptors." *Mol. Pharmacol.* **39**:211-221.

81. Powell S.K., Rivas R.J., Rodriguez-Boulan E., hatten M.E. (1997). “Development of polarity in cerebellar granule neurons.” *J. neurobiol.* **32**:223-236.

82. Rapoport T.A. (2007). "Protein translocation across the eukaryotic endoplasmic reticulum and bacterial plasma membranes." *Nature.* **450**:663-669.

83. Rasband M.N. (2010). “The axon initial segment and the maintenance of neuronal polarity.” *Nat. Rev. Neurosci*. **11**:552-62.

84. Ridley A.J. (2001). “Rho GTPases and cell migration. *J. Cell Sci.* **114**:2713-2722.

85. Rodriguez-Boulan E., Kreitzer G., Musch A. (2005). "Organization of vesicular trafficking in epithelia." *Nat Rev. Mol. Cell Biol.* **6**:233-247.

86. Salahpour A., Angers S., Mercier J.F., Lagacé M., Marullo S., and Bouvier M. (2004). "Homodimerization of the beta2-adrenergic receptor as a prerequisite for cell surface targeting." *J. Biol. Chem.* **279**:33390-33397.

87. Sanchez-Ponce D., Tapia M., Munoz A., and Garrido J.J. (2008). “New role for IKK α/β phosphorylated IκBα in axon outgrowth and axon initial segment development.” *Mol. Cell Neurosci.* **37**:832-844

88. Sarnataro D., Paladin S., campana V., Grassi J., Nitsch L., Zurzolo C. (2002). “PrPC is sorted to the basolateral membrane of epithelial cells independently of its association with rafts.” *Traffic*. **3**:810-821.

89. Scheiffele P., Roth M.G., Simons K. (1997).”Interaction of influenza virus haemagglutinin with spingolipid-cholesterol membrane domains via its transmembrane domain.” *EMBO J.* **16**:5501-5508.

90. Scherer N.M. and Nathanson N.M. (1990). "Differential regulation by agonist and phorbol ester of cloned m1 and m2 muscarinic receptors in mouse Y1 adrenal cells and in Y1 cells deficient in cAMP-dependent protein kinase." *Biochemsitry*. **29**:8475-8483.

91. Schoenenberger C., Mannherz H.G., and Jockusch B.M. (2011). “Actin: From structural plasticity to functional diversity.” *Europ. J. of Cell Biol.* **90(10)**:797-804.

92. Sheff D.R., Kroschewski R., Mellman I. (2002). "Actin dependence of polarized receptor recycling in Mardin-Darby canin kidney cell endosomes." *Mol. Biol. Cell.* **13**:262-275.

93. Shi S.H., Jan L.Y., and Jan Y.N. (2003). “Hippocampal neuronal polarity specified by spatially localized mPar3/mPar6 and PI 3-kinase activity.” *Cell.* **112**:63-75.

94. Shin D.M., Luo X., Wilkie T.M., Miller L.J., Peck A.B., Humphreys-Beher M.G., and Muallem S. (2001). "Polarized expression of G protein-coupled receptors and an all-or-none discharge of Ca2+ pools at initiation sites of [Ca2+]i waves in polarized exocrine cells." *J. Biol. Chem.* **276**:44146-44156.

95. Shmuel M., Nodel-Berner E, Hyman T., Roubinski A., and Altschuler Y. (2007). "Caveolin 2 regulates endocytosis and trafficking of the M1 muscarinic receptor in MDCK epithelial cells." *Mol. Biol. Cell.* **18**:1570-1585.

96. Simon S.A. and Baggett H.C. (1992). "Identification of muscarinic acetylcholine receptors in istolated canine lingual epithelia via voltage clamp measurements." *Arch. Oral Biol.* **37**:685-690.

97. Simons K., van Meer G. (1988). "Lipid sorting in epithelial cells." *Biochemistry*. **27**:6197-6202.

98. Song A.H., Wang D., Chen G., Li Y., Luo J., Duan S., and Poo M.M. (2009). "A selective filter for cytoplasmic transport at the axon initial segment." *Cell*. **136**:1148-60.

99. St. Johnston D., Ahringer J. (2010). "Cell polarity in eggs and epithelia: parallels and diversity." *Cell*. **141**:757-774.

100. Surma M.A., Klose C., Klemm R.W., Ejsing C.S., Simons K. (2011). "Generic sorting of raft lipids into secretory vesciles in yeast." *Traffic*. **12**:1139-1147.

101. Tahirovic S. and Bradke F. (2009). "Neuronal Polarity." *Cold Spring Harb. Perspect. Biol.* **1**:a001644s.

102. Takeuchi T., Fujinami K., Goto H., Fujita A., Taketo M.M., Manabe T., Matsui M., and Hata F. (2005). "Roles of M2 and M4 muscarinic receptors in regulating acetylcholine release from myenteric neurons of mouse ileum." *J. Neurophysiol.* **93**:2841-2848.

103. Tolbert L.M. and Lameh J. (1986). "Human muscarinic cholingergic receptor Hm1 internalizes via clathrin-coated vesicles." *J. Biol. Chem.* **271**:17335-17342.

104. Tsuga H., Kameyama K., Haga T., Honma T., Lameh J., and Sadée W. (1998). "Internalization and down-regulation of human muscarinic acetylcholine receptor m2 subtypes. Role of third intracellular m2 loop and G protein-coupled receptor kinase 2." *J. Biol. Chem.* **273**:5323-5330.

105. Vagin O., Turdikulova S., Sachs G. (2005). “Recombinant addition of *N*-glycosylation sites to the basolateral Na,K-ATPase beta1 subunit results in its clustering in caveolae and apical sorting in HGT-1 cells.” *J. Biol. Chem.* **280**:43159-43167.

106. van Koppen C.J., Kaiser B. (2003). "Regulation of muscarinic acetylcholine receptor signaling." *Pharmacol. Ther.* **98(2)**:197-220.

107. van Meer G., Simons K., (1986). "The function of tight junctions in maintaining differences in lipid composition between the apical and the basolater cell surface domains of MDCK cells." *EMBO*. **5**:1455-1464.

108. Vitriol E.A. and Zheng J.Q. (2012). “Growth Cone Travel in Space and Time: the Cellular Ensemble of Cytoskeleton, Adhesion, and Membrane.” *Neuron*. **(73)6**:1068-1081.

109. Wehrle-Haller B., Imhof B.A. (2001). "Stem cell factor presentation to c-Kit. Identification of a basolateral targeting domain." *J. Biol. Chem.* **276(16)**:12667-74.

110. Weisz O.A., Rodriguez-Boulan E. (2009). “Apical trafficking in epithelial cells: signals, clusters and motors.” *J. Cell. Sci.* **122**:4253-4266.

111. Wickman K., Clapham D.E. (1994). "Ion channel regulation by G proteins." *Phisiol. Rev.* **75**:865-885.

112. Winckler B., Forscher P., and Mellman I. (1999). "A diffusion barrier maintains distribution of membrane proteins in polarized neurons." *Nature*. **397**:698-701.

113. Witte H. and Bradke F. (2008). “The role of the cytoskeleton during neuronal polarization.” *Curr. Opin. Neurobiol*. **18**:479-487.

114. Witte H., Neukirchen D., and Bradke F. (2008). “Microtubule stabilization specifies initial neuronal polarization.” *J. Cell Biol.* **180**:619-632.

115. Wittmann T., Bokoch G.M., and Waterman-Storer C.M. (2004). “Regulation of microtubule destabilizing activity of Op18/stathmin downstream of Rac1.” *J. Biol. Chem.* **279**:6196-6203.

116. Yamanaka T., Ohno S. (2008). "Role of Lgl/Dlg/Scribble in the regulation of epithelial junction, polarity, and growth." *Font. Biosci.* **13**:6693-6707.

117. Yang Y., Ogawa Y., Hedstrom K.L., and Rasband M.N. (2007). "betaIV spectrin is recruited to axon initial segments and nodes of Ranvier by ankyrin G." *J. Cell Biol.* **176**:509-519.

118. Yeaman C., Le Gall A.H., Baldwin A.N., Monlauzeur L., Le Bivic A., Rodriguez-Boulan E. (1997). "The *O*-glycosylated stalk domain is required for apical sorting of neurotrophin receptors in polarized MDCK cells." *Traffic.* **139**:929-940.

119. Zurzolo C., Lisanti M.P., Caras I.W., Nitsch L., Rodriguez-Boulan E. (1993). "Glycosylphosphotidylinositol-anchored proteins are preferentially targeted to the basolateral surface in Fischer rat thyroid epithelial cells." *J. Cell Biol.* **121**:1031-1039.